Published OnlineFirst February 24, 2009; DOI: 10.1158/0008-5472.CAN-08-1808

Research Article

# Sonic Hedgehog Signaling Pathway Is Activated in ALK-Positive Anaplastic Large Cell Lymphoma

Rajesh R. Singh,[1] Jeong Hee Cho-Vega,[1] Yogesh Davuluri,[1] Shuguang Ma,[1] Fatan Kasbidi,[1] Cristiane Milito,[1] Patrick A. Lennon,[2] Elias Drakos,[1] L. Jeffrey Medeiros,[1] Rajyalakshmi Luthra,[1] and Francisco Vega[1]

Department of [1]Hematopathology and [2]School of Health Sciences, The University of Texas M. D. Anderson Cancer Center, Houston, Texas

## Abstract

**Deregulation of the sonic hedgehog (SHH) signaling pathway has been implicated in several cancers but has not been explored in T-cell lymphomas. Here, we report that the SHH/GLI1 signaling pathway is activated in anaplastic lymphoma kinase (ALK)–positive anaplastic large cell lymphoma (ALCL). We show that *SHH*, but not its transcriptional effector *GLI1*, is amplified in ALK+ ALCL tumors and cell lines, and that SHH and GLI1 proteins are highly expressed in ALK+ ALCL tumors and cell lines. We also show that inhibition of SHH/GLI1 signaling with cyclopamine-KAAD, as well as silencing *GLI1* gene expression by small interfering (si)RNA, decreased cell viability and clonogenicity of ALK+ ALCL cells. Transfection of wild-type or mutant NPM-ALK into 293T cells showed that only wild-type NPM-ALK increased GLI1 protein levels and activated SHH/GLI1 signaling as shown by increase of *CCND2* mRNA levels. Inhibition of ALK tyrosine kinase and phosphatidylinositol 3-kinase (PI3K)/AKT or forced expression of pAKT down-regulated or up-regulated SHH/GLI1 signaling, respectively. Inhibition of GSK3β in 293T cells also increased protein levels of GLI1. In conclusion, the SHH/GLI1 signaling pathway is activated in ALK+ ALCL. SHH/GLI1 activation is the result of *SHH* gene amplification and is further mediated by NPM-ALK through activation of PI3K/AKT and stabilization of GLI1 protein. There is a positive synergistic effect between the SHH/GLI1 and PI3K/AKT pathways that contributes to the lymphomagenic effect of NPM-ALK.** [Cancer Res 2009;69(6):2550–8]

## Introduction

Anaplastic lymphoma kinase (ALK)-positive anaplastic large cell lymphoma (ALCL) is an aggressive type of non–Hodgkin lymphoma of T-cell/null lineage (1, 2). This lymphoma is characterized by chromosomal aberrations that lead to constitutive activation of ALK. The most common is t(2;5)(p23;q35), which produces a fusion between the nucleophosmin (*NPM*) and *ALK* genes, leading to expression of the NPM-ALK fusion protein (3). NPM-ALK mediates oncogenesis, at least in part, through phosphorylation/activation of phosphatidylinositol 3-kinase (PI3K), the serine/threonine kinase AKT/mammalian target of rapamycin and Janus kinase/signal transducers and activators of transcription pathways, resulting in cell proliferation and antiapoptotic signals (4–6).

The Hedgehog protein family is a group of secreted signaling molecules that is critical for normal mammalian development. In the immune system, sonic hedgehog (SHH), is a regulator of T-cell differentiation, T-cell receptor–repertoire selection, and peripheral T-cell activation (7, 8). SHH is also one of the survival signals provided by follicular dendritic cells to prevent apoptosis in germinal center B cells (9). Although inappropriate activation of the SHH signaling pathway has been shown in many cancers (10), the role of SHH/GLI signaling pathway in T-cell lymphomas has not been explored.

SHH interacts with a receptor complex composed of two transmembrane proteins, patched (PTCH) and smoothened (SMO). PTCH is the SHH ligand–binding subunit and SMO is the signal transduction component. In the absence of SHH, PTCH inhibits SMO. Once SHH binds PTCH, this inhibition is released allowing SMO to transduce the SHH signal, mediated by the glioma-associated oncogene homologue (GLI) transcription factors (11).

Here, we show that the *SHH* gene is frequently amplified in ALK+ ALCL, and that NPM-ALK, through activation of PI3K/AKT, contributes to activation of SHH/GLI1 signaling pathway. We also show that SHH/GLI1 activation mediates cell proliferation and cell survival in ALK+ ALCL cell lines and contributes to the oncogenic effect of NPM-ALK.

## Materials and Methods

**Cell lines.** Four ALK+ ALCL cell lines (Karpas 299, SUDHL1, DEL, and SUPM2), one T-cell lymphoma/leukemia cell line (Jurkat), and one human embryonic kidney epithelial cell line (293T) were used. Cells were maintained at 37°C in RPMI 1640 (Life Technologies) supplemented with 10% fetal bovine serum (FBS; Sigma) in a humidified atmosphere containing 5% $CO_2$.

**Immunohistochemistry.** Expression of SHH and GLI1 was assessed immunohistochemically using tissue microarrays as previously described (6). In all cases, the ALK+ ALCL tumors were positive for CD30 and ALK, and the ALK-negative ALCL tumors were positive for CD30 but negative for ALK. Rabbit polyclonal antibodies for SHH (H-160) and GLI1 (H-300) were used (Santa Cruz Biotechnology). Protein expression levels were scored as negative, weakly positive, and strongly positive, depending on the staining signal intensity. A minimum of 10% of the tumor cells expressing these proteins was required to consider a neoplasm as positive.

**Real-time quantitative (q)PCR for SHH and GLI1 copy number estimation.** Copy number of *SHH* at 7q36 and *GLI1* genes at 12q13 was assessed by real-time qPCR. *Cyclophilin 40* (*CYP40*) gene was used as normalizer. The primer and probe sequences used were as follows: *GLI1*, 5′-GAC CCT GAG ATT GCC TCT CTT G-3′ (forward), 5′-CAT CCC AAC GGC AGT CAG T-3′ (reverse), and 6-FAM 5′-AGA GAG AGG AGA AGC GTG A-MGB3′ (probe); *SHH*, 5′-CCT TGA CAC CTT AAC AGT GTT TTC CTA-3′ (forward), 5′-TGG AAT TTA GGA GAC AAG TAG GGA A-3′ (reverse), and 6-FAM 5′-CTA ACA TAG TGC CAT TAA C-MGB 3′ (probe); and *CYP40*,

**Note:** Supplementary data for this article are available at Cancer Research Online (http://cancerres.aacrjournals.org/).

R.R. Singh and J.H. Cho-Vega contributed equally to this work.

**Requests for reprints:** Francisco Vega, Department of Hematopathology, Unit 72, The University of Texas M. D. Anderson Cancer Center, 1515 Holcombe Boulevard, Houston, TX 77030. Phone: 713-794-1220; Fax: 713-745-0736; E-mail: fvegava@mdanderson.org.



doi:10.1158/0008-5472.CAN-08-1808

Published OnlineFirst February 24, 2009; DOI: 10.1158/0008-5472.CAN-08-1808



5′-TGA GAC AGC AGA TAG AGC CAA GC-3′ (forward), 5′-TCC CTG CCA ATT TGA CAT CTT C-3′ (reverse), and 6-FAM 5′-AGC ACC AAT ATT CAG TAC ACA GCT TAA AGC TAT-MGB-3′ (probe). Pooled DNA derived from six to eight normal individuals was used as reference DNA. Each target was amplified individually and in duplicate. Gene copy numbers were calculated using the δ CT (ΔCT) method.

**Fluorescence *in situ* hybridization analysis.** We designed a fluorescence *in situ* hybridization (FISH) test for *SHH* using a proximal bacterial artificial chromosome clone, which included *SHH* (RP11-69O3; 155.01–155.15 MB on chromosome 7q) and a more distal clone, which also included *SHH* (RP11-161A19; 155.07–155.22 MB on chromosome 7q) as previously described (12). In essence, this produced a *SHH* red/green FISH probe. The centromere 7 probe was purchased from Abbott Laboratories and used according to the manufacturer's recommendations.

**NPM-ALK transfection.** Plasmids used to express wild-type (WT) and kinase-dead mutant NPM-ALK [lysine 210 mutated to arginine (K210R)] that lacks ability to bind to ATP, have been described previously (13). 293T cells were transfected with empty vector (pDest40), WT NPM-ALK, or kinase-dead mutant NPM/ALK plasmids using Fugene HD transfection reagent (Roche Applied Sciences) as per the manufacturer's instructions.

**Double immunofluorescence labeling and confocal microscopy.** Double immunofluorescence labeling was performed in 293T cells cultured in chamber slides (Fisher Healthcare) following the manufacturer's recommendations. Cells were incubated for 1 h at room temperature with a mouse anti-GLI1 monoclonal antibody (Cell Signaling) and a rabbit anti–total ALK polyclonal antibody (Zymed). Alexa Fluor 594 (red) goat anti-mouse IgG conjugate and Alexa Fluor 488 (green) goat anti-rabbit IgG conjugate antibodies (Molecular Probes) were used as secondary antibodies. The nuclei were stained with 4′-6′ diamidino-2-phenylindole (DAPI). Analysis was done with an Olympus FV500 confocal laser microscope.

**Western blot analysis.** Western blotting was done as described previously (6). Antibodies used were as follows: SHH, SMO, $Tyr^{216}$pGSK3β (Santa Cruz Biotechnology), GLI1 (GeneTex), $Tyr^{664}$pALK, $Thr^{308}$pAKT, total AKT, $Thr^{197}$pPKA, total PKA, $Ser^{21/9}$pGSK3α/β, total GSK3 (Cell Signaling), total ALK (Zymed), and β-actin (Sigma). Reactions were visualized with suitable secondary antibodies conjugated with horseradish peroxidase using enhanced chemiluminescence reagents (Amersham Pharmacy).

**Luciferase reporter gene assay.** A luciferase reporter plasmid with a luciferase gene downstream of eight copies of GLI1-binding sites was used (14). Transfection was done using Fugene HD transfection reagent (Roche Applied Sciences). Plasmid for β-galactosidase expression was also cotransfected in every experiment as transfection normalizer. Luciferase activity was measured 24 h posttransfection using the Luciferase assay kit (Promega), and β-galactosidase activity was measured using β-galactosidase enzyme assay kit (Promega).

**Treatments with NPM-ALK inhibitor (WHI-P154), PI3K inhibitor (LY294002), and GSK3β inhibitor IX (BIO).** Treatments of Karpas 299 and SUDHL1 cells with the ALK tyrosine kinase inhibitor, WHI-P154, and with the PI3K inhibitor, 2-(4-morpholinyl)-8-phenyl-4*H*-1-benzopyran-4-one (LY294002), (Calbiochem) were performed as described previously (6). 293T cells were treated with increasing concentrations of GSK3β-inhibitor IX (Bromoindirubin-3-oxime, BIO; Calbiochem) for 24 h.

**Adeno-myristoylated AKT adenovirus infection.** Karpas 299 cells were infected with the HA-tagged, constitutively active, adeno-myristoylated Akt adenovirus at a multiplicity of infection of 20, as described previously (6, 15). Whole cell lysates were prepared 48 h after infection. Expression of adeno-myristoylated Akt in infected cells was confirmed by Western blot analysis using the anti-HA antibody. Infection with a recombinant adenovirus construct expressing h-Gal (adeno-h-Gal) at the same multiplicity of infection was used as a control.

**Transfection of GLI1-specific siRNA.** sMARTpool *GLI1*-specific siRNA mixture and four individual *GLI1*-specific siRNA were purchased from Dharmacon, Inc. Transfections in Karpas 299, SUDHL1, and 293T cells were done by electroporation using the Nucleofector transfection kit (Amaxa Biosystems) as per the manufacturer's instructions. A negative siRNA control (Dharmacon, Inc.) was used. Whole-cell lysates were prepared 48 h after transfection.

**Cell viability, apoptosis, cell cycle, and clonogenicity assays.** Cell viability assays, for Karpas 299 and SUDHL1, were done in RPMI (2% FBS). Treatments were done with increasing concentrations of cyclopamine-KAAD (Calbiochem), an steroidal alkaloid inhibitor of SMO (16, 17), tomatidine, an alkaloid similar to cyclopamine but lacking the capacity to inhibit SMO (Calbiochem) and DMSO. Karpas 299 was also treated with SANT-1 (Sigma), a potent SHH pathway antagonist that directly binds and inhibits SMO. After 48 h, cell viability was assessed using a cell proliferation kit, Cell Titer 96 Aqueous One Solution (MTS; Promega). Annexin V staining (BD Biosciences Pharmingen) detected by flow cytometry was used to assess apoptosis according to the manufacter's instructions. Cell cycle analysis was performed using propidium iodide. Colony formation in methylcellulose (Stem Cell Technologies) was performed according to the manufacturer's instructions. Five hundred cells were initially plated and incubated in 300 μL of methylcellulose for 2 wk. Colonies were stained with p-iodonitrotetrazolium violet (Sigma) and counted. These experiments were performed in triplicate.

**Statistical analysis.** A two-sided proportion test was used to compare the expression among SHH signaling proteins in ALK+, ALK-negative ALCL, and PTCL-U tumors. Statistical calculations were done using StatView (Abacus Concepts, Inc.).

## Results

**Elevated levels of SHH and GLI1 proteins in ALK+ ALCL cell lines and tumor samples.** Expression of SHH and GLI1 was assessed immunohistochemically in 28 ALK+ ALCL tumors (Table 1). SHH was confined to the cytoplasm and was strongly positive in all cases (Fig. 1*A*). GLI1 was predominantly cytoplasmic and strongly positive in 23 of 28 (82%) cases. Although nuclear localization of GLI1 was also seen in all cases, the level of expression was lower than that detected in the cytoplasm. Small reactive lymphocytes were negative and served as internal negative control.

We also explored the expression levels of these proteins in 20 cases of ALK-negative ALCL and 18 cases of PTCL-U (Table 1).

**Table 1.** SHH and GLI1 protein expression in ALK+, ALK-negative ALCL, and PTCL-U tumors

| | ALK+ ALCL ($n$ = 28) | ALK-negative ALCL ($n$ = 20) | PTCL-U ($n$ = 18) |
|---|---|---|---|
| SHH | 28 (100%) | 17 (85%) | 1 (5.5%) |
| GLI1 | 23 (82.1%) | 2 (10%) | 1 (5.5%) |

NOTE: Only cases with strong levels of expression are shown. The differences of those proportions are statistically significant ($P < 0.000001$, two-sided proportion test).

Published OnlineFirst February 24, 2009; DOI: 10.1158/0008-5472.CAN-08-1808



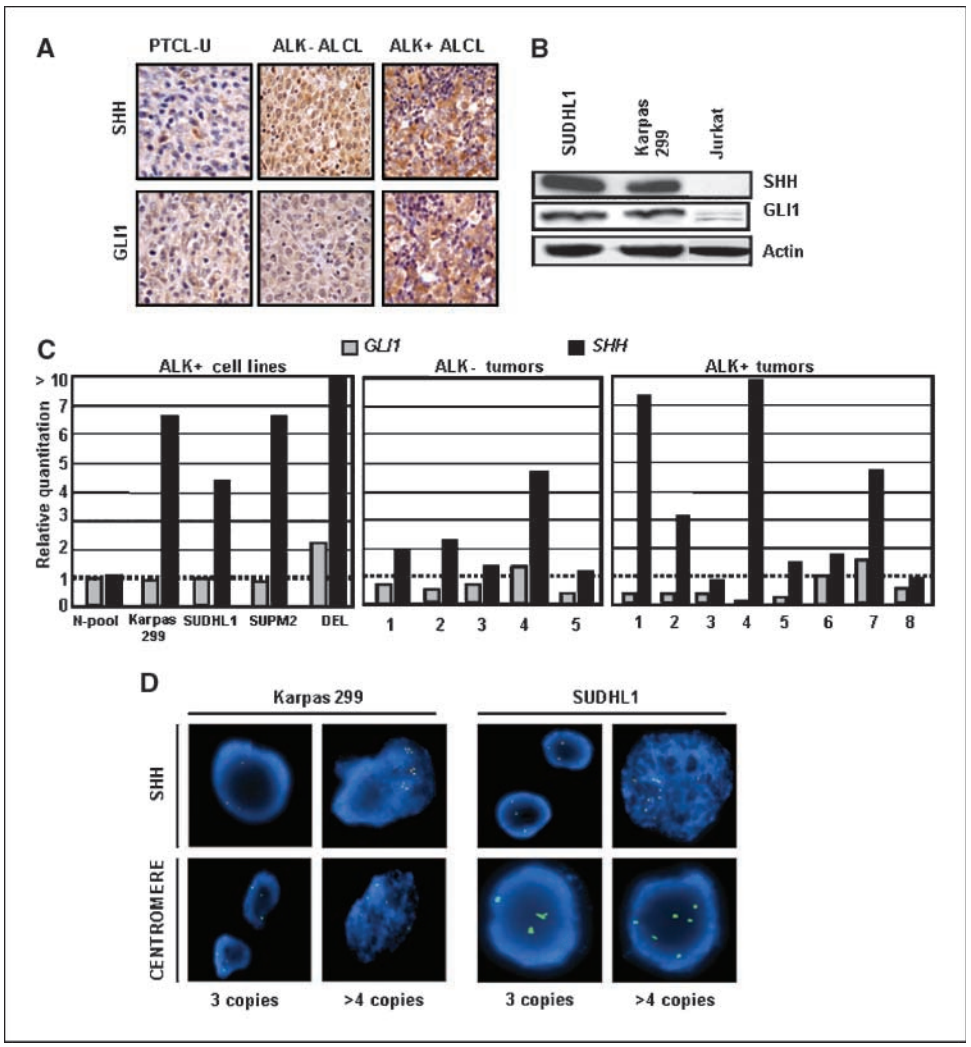


**Figure 1.** SHH/GLI1 protein levels in ALK+, ALK-negative ALCL, and PTCL-U tumors and cell lines. *A,* representative pictures of immunohistochemistry showing expression levels of SHH and GLI1. PTCL-U were characterized by low levels of expression of SHH and GLI1; ALK-negative ALCL revealed high levels of SHH, and low levels of GLI1 and ALK+ ALCL showed high expression of both proteins. *B,* Western blot analysis revealed higher expression of SHH and GLI1 proteins in Karpas 299 and SUDHL1 than Jurkat cell line. *C,* real-time qPCR gene copy number analysis. Six of 8 ALK+ ALCL tumors (patients 1, 2, 4, 5, 6, and 7), 4 of 5 ALK-negative ALCL tumors (patients 1, 2, 3, and 4), and all cell lines showed amplification of *SHH* but no amplification of *GLI1*. *D,* extra copies of *SHH* locus in Karpas 299 and SUDHL1 were confirmed using FISH. In Karpas 299, 33% of the cells had 3 copies of *SHH* and 40% of the cells had 4 or more copies of *SHH*. In SUDHL1, 22% of the cells had 3 copies of *SHH* and 55% of the cells had 4 or more copies of *SHH*.

Strong cytoplasmic expression of SHH was detected in 17 of 20 (85%) cases of ALK-negative ALCL. However, most of the ALK-negative ALCL tumors showed weak expression (cytoplasmic and nuclear) of GLI1 (Fig. 1*A*). Strong cytoplasmic levels of GLI1 were detected in only 2 of 20 (10%) cases. Expression of SHH and GLI1 was detected in 8 (44.4%) and 14 (77.7%) cases of PTCL-U, respectively, but the level of expression of both proteins was weak in almost all cases (Fig. 1*A*); only 1 (5.5%) neoplasm showed strong cytoplasmic expression of SHH and GLI1.

Western blot analysis also showed higher expression of SHH, and GLI1 in two ALK+ ALCL cell lines, Karpas 299 and SUDHL1, compared with Jurkat, further confirming the immunohistochemical results (Fig. 1*B*). These results indicate that ALK+ ALCL are characterized by high expression of SHH and GLI1, compared with other T-cell lymphomas, and that the expression of GLI1 was characteristically high in the cytoplasm of ALK+ ALCL cells.

***SHH gene*, but not *GLI1*, is amplified in ALK+ ALCL cell lines.** *SHH* and *GLI1* copy number was assessed by real-time qPCR. We detected extra copies of the *SHH* locus, but not of *GLI1*, in all 4 ALK+ ALCL cell lines, in 6 of 8 (75%) ALK+ ALCL tumors, and in 3 of 5 (60%) ALK-negative ALCL tumors (Fig. 1*C*). A loss involving the *GLI1* locus was seen in a subset of ALK+ and ALK-negative ALCL tumors but not in the cell lines.

To confirm the presence of extra copies of the *SHH* gene, FISH studies were performed. Dual-color (red/green) interphase FISH using two differently labeled, overlapping bacterial artificial chromosome probes (green and red), each of which contains *SHH* at 7q36.2, was performed in Karpas 299 and SUDHL1. FISH using a chromosome 7 centromeric probe was also performed. Extra copies of the *SHH* locus were confirmed using FISH and are, at least in part, due to the presence of aneuploidy of chromosome 7 (Fig. 1*D*).

These results suggest that the presence of extra copies of *SHH* gene may contribute to the increased levels of SHH protein observed in ALK+ ALCL cell lines and in ALK+ and ALK-negative ALCL tumor samples. However, no extra copies of *GLI1* gene were detected in ALK+ ALCL cell lines and/or tumors. Thus, amplification of *GLI1* is not the factor behind the high levels of GLI1 protein detected in ALK+ ALCL tumors and cell lines.

**NPM-ALK induces cellular accumulation of GLI1.** To assess the role of NPM-ALK in the activation of SHH/GLI1 signaling, we treated Karpas 299 and SUDHL1 with increasing concentrations of WHI-P154, an inhibitor of the tyrosine kinase activity of ALK (18). Increasing concentrations of WHI-P154 resulted in a concentration-dependent decrease of pALK, indicating inhibition of its kinase activity. A progressive decrease in the total protein levels of

Published OnlineFirst February 24, 2009; DOI: 10.1158/0008-5472.CAN-08-1808



GLI1 and SHH was also observed (Fig. 2*A*). This was also confirmed using double immunofluorescence and confocal microscopic examination in Karpas 299 (Fig. 2*A, bottom right*). These findings suggest that NPM-ALK increases the cellular levels of GLI1 and that this effect is dependent on the tyrosine kinase activity of ALK.

To further study if NPM-ALK contributes in the activation of SHH/GLI1 signaling, we transiently overexpressed WT NPM-ALK into 293T. Transfection of WT NPM-ALK resulted in increased cellular levels of GLI1 as detected by confocal microscopy analysis, in comparison with the untransfected cells (Fig. 2*B, left four panels*). No increase in GLI1 levels was seen on transfecting kinase-dead NPM-ALK protein (K210R), implicating the kinase activity of ALK in increasing GLI1 levels (Fig. 2*B, right four panels*). This was further confirmed by Western blotting analysis (Fig. 2*C*).

These findings indicate that NPM-ALK is involved in the increase of the cellular levels of GLI1 protein seen in ALK+ ALCL, which in combination with the increased SHH protein levels contributes to the activation of this pathway in this lymphoma type.

**NPM/ALK modulates SHH/GLI1 levels through activation of PI3K/AKT.** NPM-ALK mediates oncogenesis, at least in part, through activation of PI3K/AKT signaling pathway (19). To study the contribution of PI3K/AKT signaling pathway in the activation of SHH/GLI1 pathway, first, we inhibited PI3K using increasing concentrations of LY294002 (4). Inhibition of PI3K led to a concentration-dependent decrease of SHH and GLI1 protein levels in Karpas 299 cells (Fig. 3*A*). This was also accompanied by decreased levels of phosphorylated/inactivated form of GSK3β, one of the molecules phosphorylated (inactivated) by AKT but not PKA (Fig. 3*A*).

To further confirm the role of AKT in the activation of SHH/GLI1 pathway, we infected Karpas 299 with an adenoviral vector, adeno-myristoylated AKT, expressing constitutively active AKT (6, 15). Constitutive activation of AKT resulted in a substantial increase of SHH, GLI1, and pGSK3β (Fig. 3*B*). These results show a direct role for PI3K/AKT in regulating SHH and GLI1 protein levels in ALK+ ALCL cell lines.

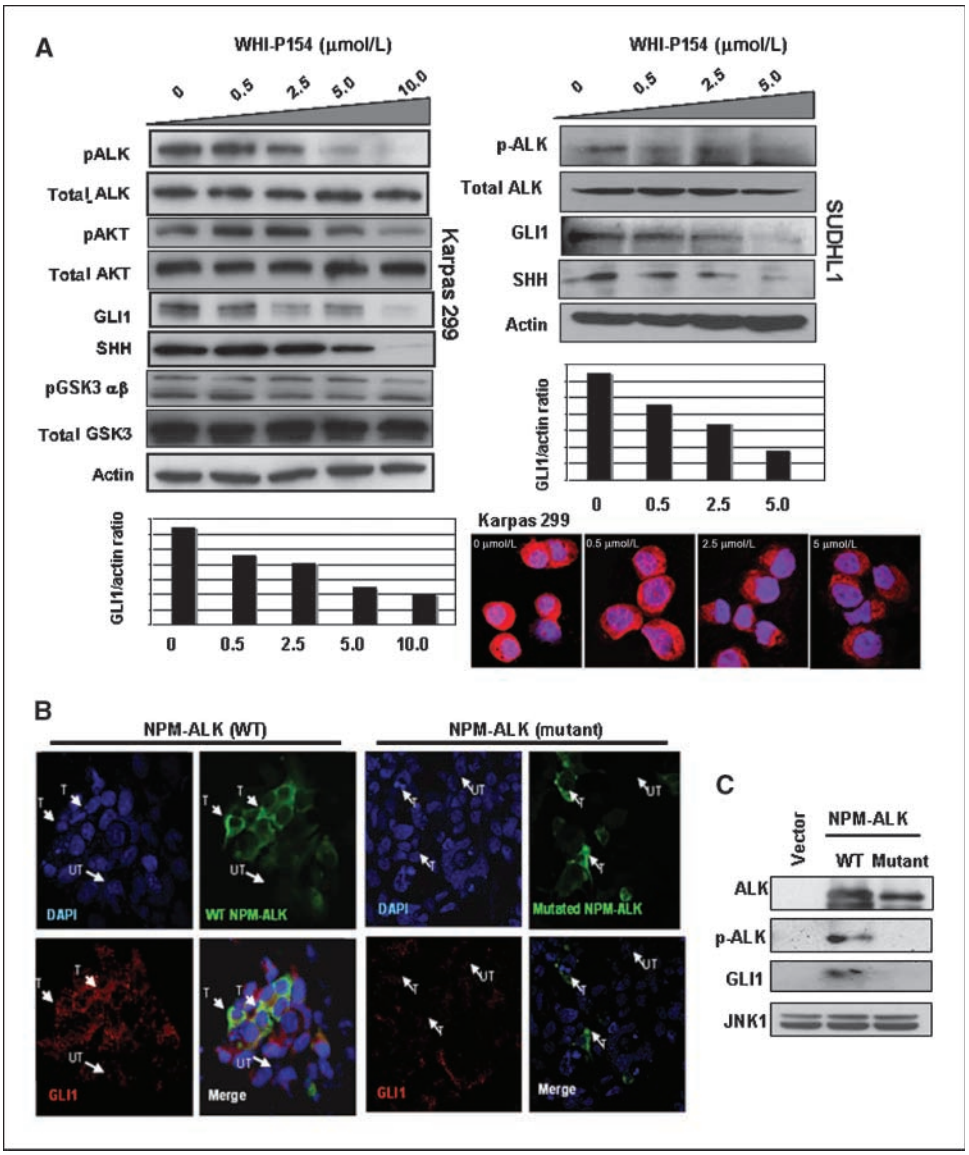


**Figure 2.** NPM-ALK chimeric protein induces cellular accumulation of GLI1 and activates the SHH/GLI1 signaling pathway. *A,* treatment of Karpas 299 (*left*) and SUDHL1 (*right*) cells with increasing concentrations of WHI-P154 for 48 h resulted in a concentration-dependent decrease in the levels of SHH and GLI1. This was accompanied by a decrease in the levels of pAKT and of the inactivated form of GSK3β (*left*). The decrease of GLI1 levels after treatment of Karpas 299 cells with increasing concentrations of WHI-P154 was also confirmed using an immunofluorescence assay. *B,* transient transfection of NPM-ALK chimeric protein induced increase of GLI1 expression. Transfection of WT NPM-ALK in the 293T cell line resulted in increased expression of GLI1 protein as detected by double immunofluorescence (*left four panels*). No increase of GLI1 levels was noted when the kinase-dead (K210R) NPM/ALK was transfected (*right four panels*; *UT,* untransfected cell; *T,* transfected cell; *blue,* DAPI; *green,* WT or kinase-dead NPM-ALK; *red,* GLI1). *C,* Western blot analysis confirmed the increase in the levels of GLI1 protein after transfection of WT NPM-ALK in 293T cells. c-Jun-$NH_2$-kinase was used as protein loading control.

Published OnlineFirst February 24, 2009; DOI: 10.1158/0008-5472.CAN-08-1808



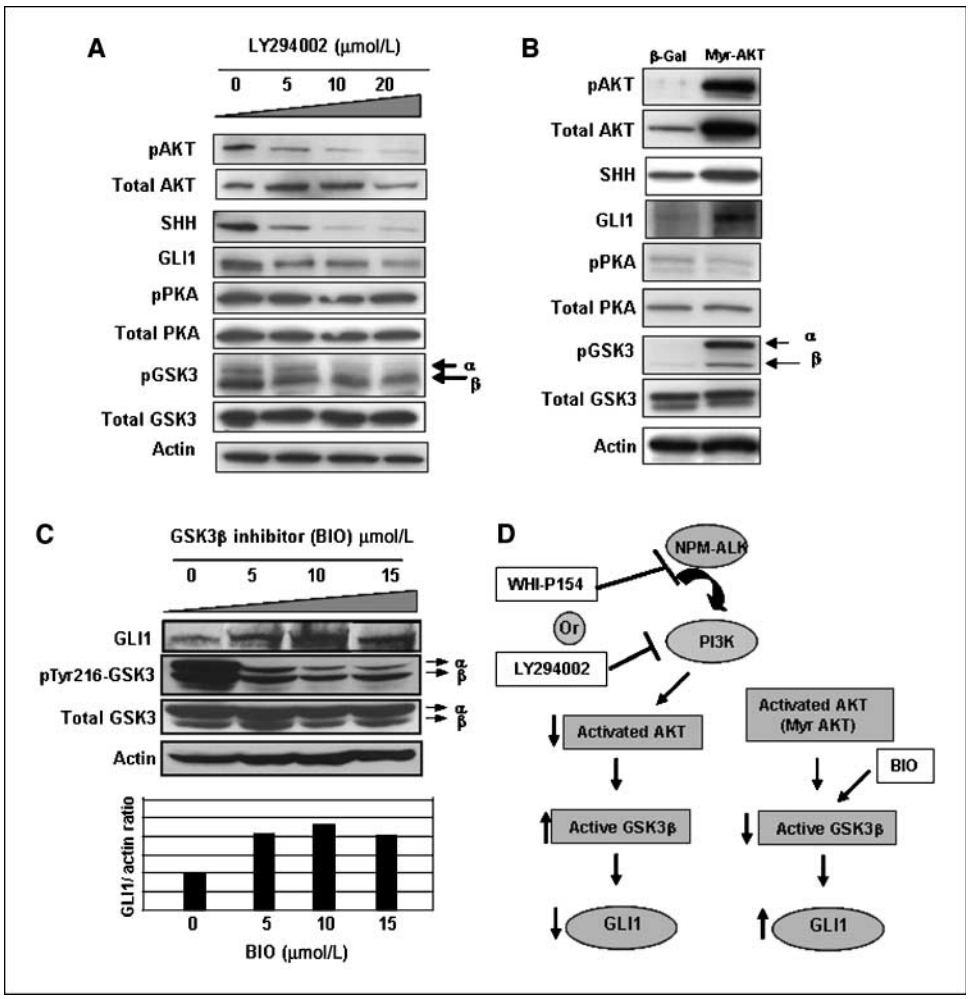


**Figure 3.** The activation status of PI3K/AKT modulates SHH/GLI1 levels. *A,* Karpas 299 cells were treated with increasing concentrations of LY294002. Western blot analysis showed concentration-dependent decrease in the levels of GLI1 and SHH proteins. A decrease in the levels of pAKT and inhibition of phosphorylation of GSK3β was also noted. *B,* AKT activation up-regulates SHH signaling proteins. Karpas 299 were infected with constitutively active adeno-myristoylated AKT adenovirus, which resulted in up-regulation of GLI1 and SHH proteins. An increase in the levels of inactivated GSK3β (pGSK3β) but not in pPKA was also noted. *C,* in 293T cells, a z'dose-dependent increase in the levels of GLI1 was observed after treatment with BIO. Inhibition of GS3Kβ is evident with the dose-dependent decrease in the levels of $pTyr^{216}$GS3K, which is a measure of its kinase activity. The increase of GLI1 is appreciated in the band density ratio of GLI1 to actin. *D,* schematic diagram summarizing the effects of modulating the activation status of the tyrosine kinase activity of ALK and PI3K/AKT on GLI1 protein levels. Inhibition of the tyrosine kinase activity of ALK and PI3K decreased the levels of pGSK3β and GLI1. On the contrary, the forced expression of AKT increases the levels of pGSK3β and GLI1.

GSK3β has been implicated in the proteosomal degradation of GLI2 and GLI3, but its role in GLI1 degradation is unclear (20, 21). Our results indicate that GSK3β may also be involved in regulating the stability of GLI1 protein. Inhibition of the PI3K/AKT pathway resulted in a decrease of pGSK3β (inactivated form) associated with decrease of GLI1 protein levels, and forced expression of AKT resulted in increased pGS3Kβ associated with an increase of GLI1 protein levels (Fig. 3*A* and *B*). To assess the potential role of GSK3β in modulating the stability of GLI1 protein, we studied the effect of inhibiting GSK3β kinase activity, using GSK3β inhibitor IX (BIO), on the GLI1 protein levels in 239T cells. Increasing concentrations of BIO resulted in a concentration-dependent increase of GLI1 protein levels (Fig. 3*C*), indicating that GSK3β might also be involved in the stability of GLI1 protein. The activation status of GSK3β was measured by examining the phosphorylation status of the Tyr216 residue using a phospho-specific antibody. Tyr216 is a site of autophosphorylation that results in the stimulation of its kinase activity and hence can be used as a reflection of GSK3β activity (22). A schematic diagram summarizing the effects of modulating the activation status of the tyrosine kinase activity of ALK, PI3K/AKT, and GSK3β on GLI1 levels is shown in Fig. 3*D*.

**NPM-ALK enhances the transcriptional activity of GLI1 and activates SHH/GLI1 pathway.** A luciferase assay was used to further confirm that NPM-ALK is responsible for the increase of GLI1 levels. A reporter plasmid with a luciferase gene, hepatocyte nuclear factor-3β (*HNF3β*) floor plate enhancer, whose transcriptional activity is under control of upstream GLI1-binding sites (14) was transfected into 293T cells. Cotransfection of WT NPM-ALK resulted in more than a 3-fold increase in the luciferase activity compared with the vector control and the kinase-dead NPM-ALK (Fig. 4*A*).

*CCND2* is an immediate downstream transcriptional target of GLI1 (23). Using GLI1-specific siRNA, we silenced *GLI1* expression at 48 hours by >25% in Karpas 299 and 65% in SUDHL1, respectively (Fig. 4*B, left*). This knockdown of *GLI1* was accompanied by a concomitant decrease of *CCND2* mRNA levels by >70% and 80% in Karpas 299 and SUDHL1 (Fig. 4*B, right*), respectively. Similarly, treatment of Karpas 299 with 1 μmol/L of WHI-P154 and with 10 μmol/L of cyclopamine-KAAD resulted in a decrease of 60% and 40%, respectively, of the *CCND2* mRNA levels (Fig. 4*C, left*). On the other hand, transient transfection of NPM-ALK into 293T cells resulted in almost a 4-fold increase of *CCND2* at 48 hours compared with 293T cells transfected with the vector or with the kinase-dead form of NPM-ALK (Fig. 4*C, right*). These findings confirm that NPM-ALK increases the cellular levels of GLI1 protein and activates the SHH/GLI1 signaling pathway, as shown by the increase of GLI1-responsive luciferase activity and the levels of *CCND2*.

**Inhibition of SHH/GLI1 signaling pathway results in decreased cell viability, colony formation, and induces cell cycle arrest in ALK+ ALCL cell lines.** Treatment of Karpas 299

Published OnlineFirst February 24, 2009; DOI: 10.1158/0008-5472.CAN-08-1808



and SUDHL1 with cyclopamine-KAAD (10 μmol/L) for 48 hours decreased cell viability by 20% to 30% (Supplementary Fig. S1; Fig. 5*A*) in comparison with DMSO and tomatidine. Similar effects were obtained when we used another SMO inhibitor, SANT-1 (Supplementary Fig. S2). Treatment of Karpas 299 for 72 hours with SANT-1 resulted in a dose-dependent decrease of cell viability. No effect on cell viability was observed in the Jurkat cell line (Fig. 5*A*), which revealed low levels of expression of SHH and GLI1 proteins (Fig. 1*B*) supporting the absence or low level activation of the SHH/GLI1 signaling pathway. These findings were further supported by the fact that silencing the expression of *GLI1* in SUDHL1 cells resulted in 30% decrease in cell viability at 48 hours compared with the control siRNA (Fig. 5*B, left*). Similarly, silencing *GLI1* in Karpas 299 resulted in 35% to 40% decrease in cell viability at 48 h compared with the control siRNA (Fig. 5*B, right*).

Long-term treatment of Karpas 299 and SUDHL1 with increasing concentrations of cyclopamine-KAAD resulted in decreased colony formation in a dose-dependent manner. The maximum inhibitory effect on colony formation was seen at 10 μmol/L; an ~45% (Karpas 299) and a 70% (SUDHL1) decrease in clonogenicity was seen in comparison with controls (Supplementary Fig. S3; Fig. 5*C*). Little effect on colony formation was observed on Jurkat cells after inhibition with cyclopamine-KAAD. Treatment of SUDHL1 for 48 hours with 10 μmol/L cyclopamine-KAAD resulted in an increase in the percentage of cells in $G_1$ phase and in a decrease in the percentage of cells in S phase compared with the controls (Fig. 5*D*).

The decrease in cell viability of Karpas 299 and SUDHL1 observed after inhibiting SHH/GLI1 signaling was associated with increased apoptosis as determined by Annexin V staining, in a dose-dependent manner in both cell lines (Fig. 6*A* and *B*). These findings suggest that inhibition of SHH/GLI1 pathway induces apoptosis and cell cycle arrest and further support the role of SHH/GLI1 signaling pathway in the survival and proliferation of ALK+ ALCL cells.

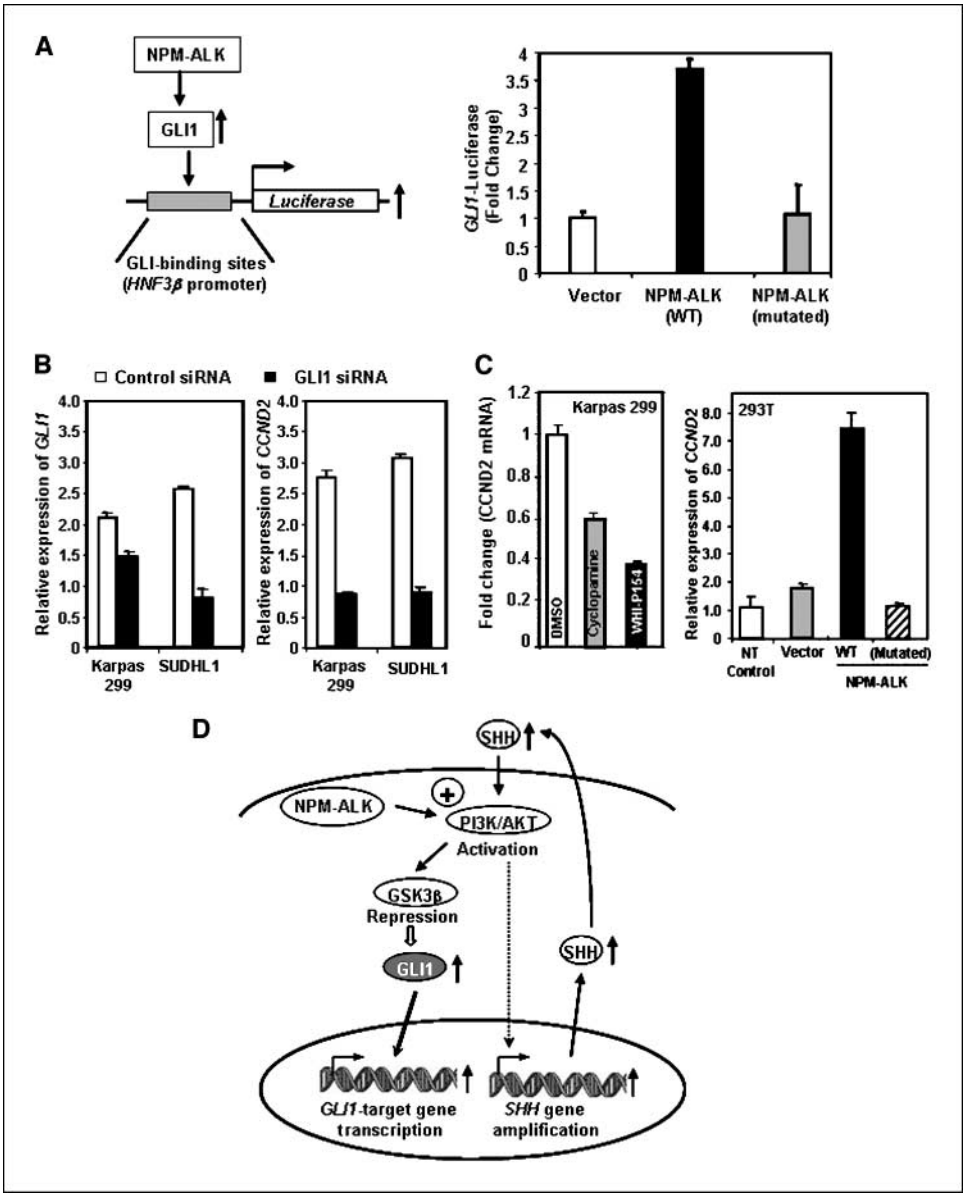


**Figure 4.** NPM-ALK enhances the transcriptional activity of GLI1. *A,* in 293T, overexpression of WT NPM-ALK resulted in a 4-fold increase of GLI1-responsive luciferase activity compared with the luciferase activity in cells transfected with the vector control. No effect was observed when the kinase-dead form of NPM-ALK was overexpressed. *B,* in Karpas 299 and SUDHL1 cells, silencing of *GLI1* expression (*left*) resulted in >3-fold decrease in the levels of *CCND2* (*right*). *C,* treatment of Karpas 299 with 1 μmol/L of WHI-P154 and 10 μmol/L of cyclopamine-KAAD resulted in a 60% and 40% decrease in the *CCND2* mRNA levels, respectively. Overexpression of NPM-ALK in 293T cells increased *CCND2* mRNA levels by 4-fold at 48 h after transfection, compared with the vector control. Similar effect was not observed by overexpressing the mutant form of NPM/ALK. *D,* proposed model to explain the positive synergistic effect between SHH/GLI1 and PI3K/AKT pathways in ALK+ ALCL.

Published OnlineFirst February 24, 2009; DOI: 10.1158/0008-5472.CAN-08-1808



## Discussion

Constitutive activation of the SHH/GLI signaling pathway by point mutations in *PTCH* or *SMO* have been associated with medulloblastoma, basal cell carcinoma, and rhabdomyosarcoma, and autocrine or paracrine pathway activation has been described for other solid tumors and B-cell malignancies but not in T-cell lymphomas (24–29). Emerging evidence is implicating the family of hedgehog proteins in the proliferation of hematopoietic stem cells, normal development of lymphoid cells, and their malignancies. For instance, SHH was found to be produced by follicular dendritic cells in the lymph node and to be necessary for the survival, proliferation, and antibody production of germinal center B cells (30). Recently, Dierks and colleagues (29) have also shown that stromally induced SHH is also an important survival signal for B-cell and plasma cell malignancies.

Here, we show, for the first time, that the SHH/GLI1 signaling pathway is activated in ALK+ ALCL. We also show the presence of extra copies of the *SHH* gene but not *GLI1* in ALK+ ALCL cell lines and tumors, and that SHH and GLI1 proteins are detected at high levels in ALK+ ALCL tumors and cell lines in comparison with other T-cell lymphomas including ALK-negative ALCL. Extra copies of the *SHH* gene were also detected in 3 (60%) of 5 ALK-negative ALCL tumors. The presence of extra *SHH* gene copies may contribute, at least in part, to the increased levels of SHH protein observed in ALK+ ALCL cell lines and in ALK+ and ALK-negative ALCL tumor samples.

To our knowledge, extra copies of the *SHH* locus have not been previously reported in PTCL-U or ALK+ ALCL. However, gains in chromosome 7 have been reported relatively frequently in lymphomas including PTCL-U and ALCL (31, 32). Zettl and colleagues (31) reported gains of chromosomal material at 7q22-qter in 31% of cases of PTCL-U, and at 7q34-qter in 1 of 9 (11%) cases of ALK+ ALCL. The genes involved were not further specified. More recently, Nagel and colleagues (33) described an amplification involving 7q22 in the SUDHL1 cell line, and identified the cyclin-dependent kinase 6 (*CDK6*) as one of the genes involved in the amplification.

We provide evidence that activation of the SHH/GLI1 pathway is enhanced by activation of the PI3K/AKT signaling pathway by NPM-ALK and that the accumulation of GLI1 may be the result of increased protein stability, as result of inactivation of GSK3β by AKT. Previously, it has been shown that NPM-ALK protein mediates oncogenesis, at least in part, through phosphorylation/activation of AKT, a downstream effector of PI3K (4, 19). Several studies have found that PI3K and AKT contribute to the activation of SHH/GLI1 signaling. It has been shown that some growth factors such as platelet-derived growth factor, epidermal growth factor, and insulin like growth factor-1 increase expression of SHH protein and that this increase is dependent on PI3K and AKT activation (34–37). Yang and colleagues (34) have shown, as in our study, that adenoviral delivery of activated AKT up-regulated SHH expression. It has been shown that recombinant SHH induces activation of

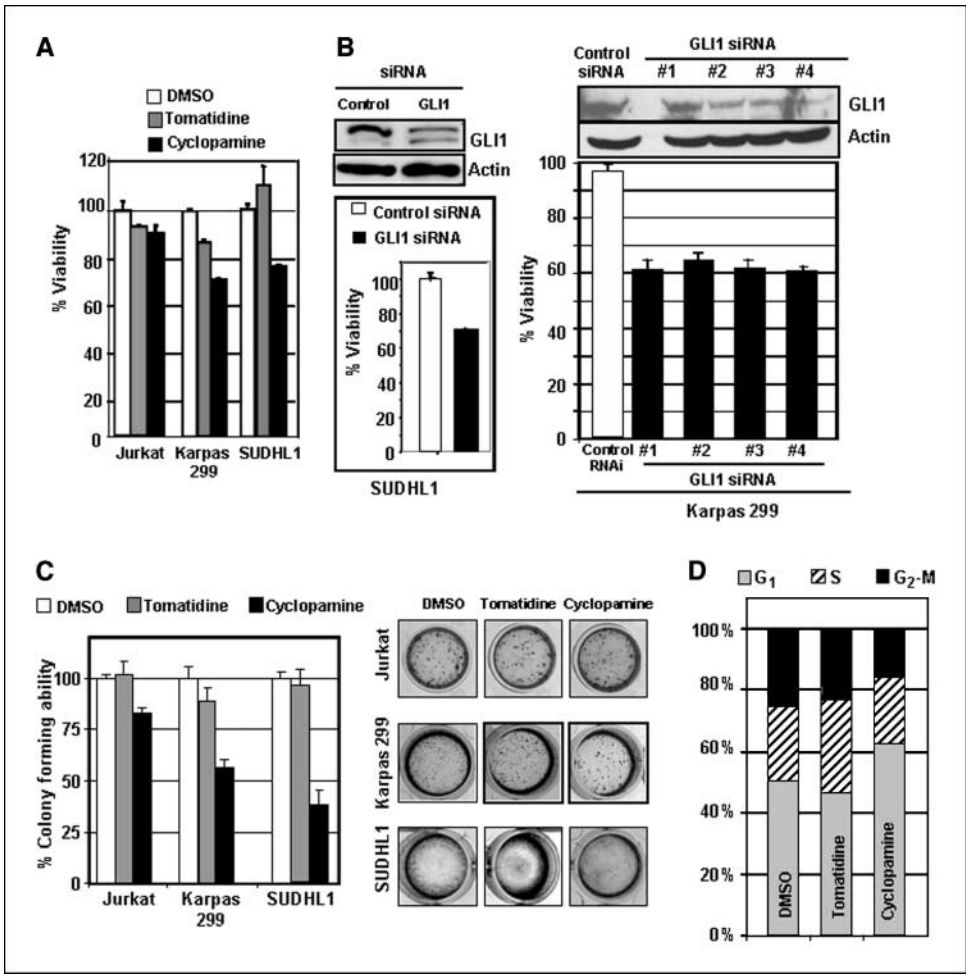


**Figure 5.** Inhibition of SHH/GLI1 signaling pathway results in decreased cell viability, colony formation, and induces cell cycle arrest in ALK+ ALCL cell lines. *A,* 48 h after treatment with 10 μmol/L cyclopamine-KAAD, the percentage of viable cells decreased by 20% to 30% in Karpas and SUDHL1 cells compared with the controls tomatidine and DMSO. No effect on viability of Jurkat cells was observed. Results shown are an average of two separate experiments. *B,* silencing of *GLI1* expression using SMARTpool siRNA and 4 individual *GLI1*-specific siRNA resulted in 30% decreased viability in SUDHL1 and Karpas 299 cells within 48 h. Successful knockdown of *GLI1* gene expression was evident in Western blots for GLI1, shown above. *C,* inhibition of SHH/GLI1 signaling with cyclopamine-KAAD decreased colony formation in 2-wk cultures of Karpas 299 (by 45%) and SUDHL1 (by 60%) compared with tomatidine and DMSO controls (*left*). Less inhibition was observed in Jurkat cells. The methylcellulose cultures stained with p-iodonitrotetrazolium violet are shown (*right*). *D,* treatment of SUDHL1 for 48 h with 10 μmol/L of cyclopamine-KAAD resulted in cell cycle arrest (cyclopamine-KAAD: $G_1$, 56.2%; S, 19.3%; $G_2$-M, 14.3%; tomatidine: $G_1$, 40.8%; S, 26.6%; $G_2$-M, 20.1%; and DMSO, $G_1$, 47.2%; S, 22.8%; $G_2$-M, 23.9%).

Published OnlineFirst February 24, 2009; DOI: 10.1158/0008-5472.CAN-08-1808



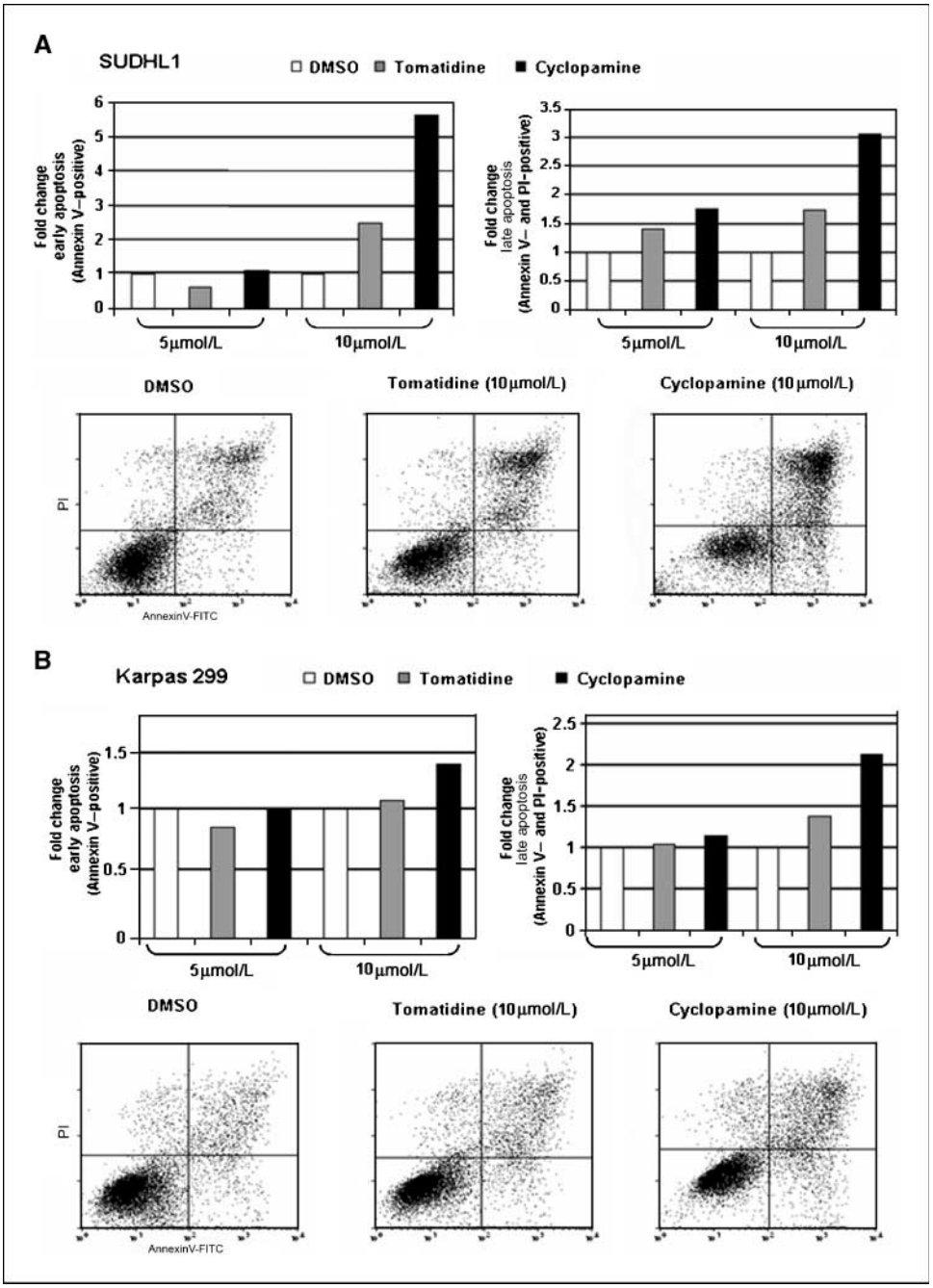


**Figure 6.** Inhibition of SHH/GLI1 signaling induces apoptosis in ALK+ ALCL cell lines. *A,* at 48 h after treatment of SUDHL1 with 10 μmol/L cyclopamine-KAAD resulted in >5-fold increase in the percentage of Annexin V–positive cells and in >3-fold increase in the percentage of Annexin V– and propidium iodide (*PI*)-positive cells (late apoptosis). *B,* in Karpas 299, this treatment resulted in 1.5-fold increase in the percentage of Annexin V–positive cells and in >2-fold increase in the percentage of Annexin V–and propidium iodide–positive cells.

PI3K/AKT (37, 38) and that LY294002 and AKT1 siRNA treatments reduce SHH-activated GLI-luciferase expression in LIGHT cells (37). In addition, genetic studies in mice have revealed that the PI3K/AKT pathway provides a synergistic signal for SHH/GLI tumor formation (39, 40). Our results also suggest that there is a synergism between PI3K/AKT and SHH/GLI1 signaling in ALK+ ALCL and that the activation of AKT contributes to the activation of the SHH/GLI1 signaling pathway.

However, the precise mechanisms by which PI3K/AKT regulates SHH/GLI1 signaling remain unclear. There is evidence that the above mentioned growth factors seem to induce SHH signaling by at least two mechanisms, increasing directly SHH ligand expression and prolonging the half-life of transcriptional effectors of SHH, such as the GLI proteins (37, 41). Earlier reports have also shown that the AKT downstream molecule GSK3β is inactivated through phosphorylation of a single serine residue by AKT (42). It has been shown that this AKT-induced inactivation of GSK3β, results in the decrease of GSK3β-mediated proteosomal degradation of GLI2 and GLI3 (21, 37). However, little is known regarding the proteosomal degradation of GLI1 in mammals.

Here, we provide preliminary evidence that GSK3β may also involved in the stability of GLI1 protein as blocking of GSK3β-kinase activity resulted in a dose-dependent increase of GLI1 protein levels, whereas inhibition of PKA resulted in no significant changes of GLI1 levels (data not shown). Our data suggest that inactivation of GSK3β by AKT, mediated by NPM-ALK, stabilizes

Published OnlineFirst February 24, 2009; DOI: 10.1158/0008-5472.CAN-08-1808



GLI1 protein resulting in the accumulation of GLI1 protein, and contribute, at least in part, to the activation of the SHH/GLI1 signaling in ALK+ ALCL. A schematic diagram summarizing the proposed positive synergistic effect between SHH/GLI1 and PI3K/AKT in ALK+ ALCL is shown in Fig. 4*D*. We also show that the SHH/GLI1 pathway is functional in ALK+ ALCL and that the inhibition of this pathway induces apoptosis and cell cycle arrest and decreased clonogenicity in ALK+ ALCL cell lines. These findings suggest that SHH/GLI1 signaling might have an autocrine role that contributes to the cell survival and proliferation in ALK+ ALCL.

In summary, SHH/GLI1 signaling pathway is activated in ALK+ ALCL. We show that the *SHH* gene is amplified in ALK+ ALCL, and that NPM/ALK, through activation of PI3K/AKT, contributes to the activation of the SHH/GLI1 signaling pathway. We propose that the accumulation of cellular GLI1 is also the result, at least in part, of its increased protein stabilization as result of inactivation of GSK3β by AKT. We also show that SHH/GLI1 activation contributes to the oncogenic effect of NPM/ALK. Our data suggest that inhibition of SHH/GLI1 signaling, in combination with blocking NPM-ALK and/or PI3K/AKT pathway, may represent a valid therapeutic approach in ALK+ ALCL.

## Disclosure of Potential Conflicts of Interest

No potential conflicts of interest were disclosed.

## Acknowledgments

Received 5/13/2008; revised 12/10/2008; accepted 1/7/2009; published OnlineFirst 2/24/2009.

The costs of publication of this article were defrayed in part by the payment of page charges. This article must therefore be hereby marked *advertisement* in accordance with 18 U.S.C. Section 1734 solely to indicate this fact.

We thank Professor Hiroshi Sasaki, Laboratory of Development Biology, Institute for Molecular and Cellular Biology, Osaka University, Japan for the GLI-responsive luciferase construct; Dr George Z Rassidakis for providing the adeno-myristoylated AKT constructs and reagents; and Dr. Hesham Amin for the critical review of this manuscript.

## References

1. Medeiros LJ, Elenitoba-Johnson KS. Anaplastic large cell lymphoma. Am J Clin Pathol 2007;127:707–22.
2. Amin HM, Lai R. Pathobiology of ALK+ anaplastic large-cell lymphoma. Blood 2007;110:2259–67.
3. Duyster J, Bai RY, Morris SW. Translocations involving anaplastic lymphoma kinase (ALK). Oncogene 2001;20:5623–37.
4. Slupianek A, Nieborowska-Skorska M, Hoser G, et al. Role of phosphatidylinositol 3-kinase-Akt pathway in nucleophosmin/anaplastic lymphoma kinase-mediated lymphomagenesis. Cancer Res 2001;61:2194–9.
5. Amin HM, McDonnell TJ, Ma Y, et al. Selective inhibition of STAT3 induces apoptosis and G(1) cell cycle arrest in ALK-positive anaplastic large cell lymphoma. Oncogene 2004;23:5426–34.
6. Vega F, Medeiros LJ, Leventaki V, et al. Activation of mammalian target of rapamycin signaling pathway contributes to tumor cell survival in anaplastic lymphoma kinase-positive anaplastic large cell lymphoma. Cancer Res 2006;66:6589–97.
7. Outram SV, Varas A, Pepicelli CV, Crompton T. Hedgehog signaling regulates differentiation from double-negative to double-positive thymocyte. Immunity 2000;13:187–97.
8. Rowbotham NJ, Hager-Theodorides AL, Cebecauer M, et al. Activation of the Hedgehog signaling pathway in T-lineage cells inhibits TCR repertoire selection in the thymus and peripheral T-cell activation. Blood 2007;109:3757–66.
9. Sacedon R, Varas A, Hernandez-Lopez C, et al. Expression of hedgehog proteins in the human thymus. J Histochem Cytochem 2003;51:1557–66.
10. Taipale J, Beachy PA. The Hedgehog and Wnt signalling pathways in cancer. Nature 2001;411:349–54.
11. Murone M, Rosenthal A, de Sauvage FJ. Hedgehog signal transduction: from flies to vertebrates. Exp Cell Res 1999;253:25–33.
12. Vega F, Cho-Vega JH, Lennon PA, et al. Splenic marginal zone lymphomas are characterized by loss of interstitial regions of chromosome 7q, 7q31.32 and 7q36.2 that include the protection of telomere 1 (POT1) and sonic hedgehog (SHH) genes. Br J Haematol 2008;142:216–26.
13. Leventaki V, Drakos E, Medeiros LJ, et al. NPM-ALK oncogenic kinase promotes cell-cycle progression through activation of JNK/cJun signaling in anaplastic large-cell lymphoma. Blood 2007;110:1621–30.
14. Sasaki H, Hui C, Nakafuku M, Kondoh H. A binding site for Gli proteins is essential for HNF-3β floor plate enhancer activity in transgenics and can respond to Shh *in vitro*. Development 1997;124:1313–22.
15. Fujio Y, Guo K, Mano T, Mitsuuchi Y, Testa JR, Walsh K. Cell cycle withdrawal promotes myogenic induction of Akt, a positive modulator of myocyte survival. Mol Cell Biol 1999;19:5073–82.
16. Taipale J, Chen JK, Cooper MK, et al. Effects of oncogenic mutations in Smoothened and Patched can be reversed by cyclopamine. Nature 2000;406:1005–9.
17. Berman DM, Karhadkar SS, Hallahan AR, et al. Medulloblastoma growth inhibition by hedgehog pathway blockade. Science 2002;297:1559–61.
18. Amin HM, Medeiros LJ, Ma Y, et al. Inhibition of JAK3 induces apoptosis and decreases anaplastic lymphoma kinase activity in anaplastic large cell lymphoma. Oncogene 2003;22:5399–407.
19. Bai RY, Ouyang T, Miething C, Morris SW, Peschel C, Duyster J. Nucleophosmin-anaplastic lymphoma kinase associated with anaplastic large-cell lymphoma activates the phosphatidylinositol 3-kinase/Akt antiapoptotic signaling pathway. Blood 2000;96:4319–27.
20. Frame S, Cohen P. GSK3 takes centre stage more than 20 years after its discovery. Biochem J 2001;359:1–16.
21. Pan Y, Bai CB, Joyner AL, Wang B. Sonic hedgehog signaling regulates Gli2 transcriptional activity by suppressing its processing and degradation. Mol Cell Biol 2006;26:3365–77.
22. Cole A, Frame S, Cohen P. Further evidence that the tyrosine phosphorylation of glycogen synthase kinase-3 (GSK3) in mammalian cells is an autophosphorylation event. Biochem J 2004;377:249–55.
23. Yoon JW, Kita Y, Frank DJ, et al. Gene expression profiling leads to identification of GLI1-binding elements in target genes and a role for multiple downstream pathways in GLI1-induced cell transformation. J Biol Chem 2002;277:5548–55.
24. Beachy PA, Karhadkar SS, Berman DM. Tissue repair and stem cell renewal in carcinogenesis. Nature 2004;432:324–31.
25. Oro AE, Higgins KM, Hu Z, Bonifas JM, Epstein EH, Jr., Scott MP. Basal cell carcinomas in mice overexpressing sonic hedgehog. Science 1997;276:817–21.
26. Watkins DN, Berman DM, Baylin SB. Hedgehog signaling: progenitor phenotype in small-cell lung cancer. Cell Cycle 2003;2:196–8.
27. Karhadkar SS, Bova GS, Abdallah N, et al. Hedgehog signalling in prostate regeneration, neoplasia and metastasis. Nature 2004;431:707–12.
28. Thayer SP, di Magliano MP, Heiser PW, et al. Hedgehog is an early and late mediator of pancreatic cancer tumorigenesis. Nature 2003;425:851–6.
29. Dierks C, Grbic J, Zirlik K, et al. Essential role of stromally induced hedgehog signaling in B-cell malignancies. Nat Med 2007;13:944–51.
30. Sacedon R, Diez B, Nunez V, et al. Sonic hedgehog is produced by follicular dendritic cells and protects germinal center B cells from apoptosis. J Immunol 2005;174:1456–61.
31. Zettl A, Rudiger T, Konrad MA, et al. Genomic profiling of peripheral T-cell lymphoma, unspecified, and anaplastic large T-cell lymphoma delineates novel recurrent chromosomal alterations. Am J Pathol 2004;164:1837–48.
32. Ott G, Katzenberger T, Siebert R, et al. Chromosomal abnormalities in nodal and extranodal CD30+ anaplastic large cell lymphomas: infrequent detection of the t(2;5) in extranodal lymphomas. Genes Chromosomes Cancer 1998;22:114–21.
33. Nagel S, Leich E, Quentmeier H, et al. Amplification at 7q22 targets cyclin-dependent kinase 6 in T-cell lymphoma. Leukemia 2008;22:387–92.
34. Yang L, Wang Y, Mao H, et al. Sonic hedgehog is an autocrine viability factor for myofibroblastic hepatic stellate cells. J Hepatol 2008;48:98–106.
35. Omenetti A, Yang L, Li YX, et al. Hedgehog-mediated mesenchymal-epithelial interactions modulate hepatic response to bile duct ligation. Lab Invest 2007;87:499–514.
36. Stepan V, Ramamoorthy S, Nitsche H, Zavros Y, Merchant JL, Todisco A. Regulation and function of the sonic hedgehog signal transduction pathway in isolated gastric parietal cells. J Biol Chem 2005;280:15700–8.
37. Riobo NA, Lu K, Ai X, Haines GM, Emerson CP, Jr. Phosphoinositide 3-kinase and Akt are essential for Sonic Hedgehog signaling. Proc Natl Acad Sci U S A 2006;103:4505–10.
38. Kanda S, Mochizuki Y, Suematsu T, Miyata Y, Nomata K, Kanetake H. Sonic hedgehog induces capillary morphogenesis by endothelial cells through phosphoinositide 3-kinase. J Biol Chem 2003;278:8244–9.
39. Rao G, Pedone CA, Del Valle L, Reiss K, Holland EC, Fults DW. Sonic hedgehog and insulin-like growth factor signaling synergize to induce medulloblastoma formation from nestin-expressing neural progenitors in mice. Oncogene 2004;23:6156–62.
40. Hahn H, Wojnowski L, Specht K, et al. Patched target Igf2 is indispensable for the formation of medulloblastoma and rhabdomyosarcoma. J Biol Chem 2000;275:28341–4.
41. Kenney AM, Widlund HR, Rowitch DH. Hedgehog and PI-3 kinase signaling converge on Nmyc1 to promote cell cycle progression in cerebellar neuronal precursors. Development 2004;131:217–28.
42. Cross DA, Alessi DR, Cohen P, Andjelkovich M, Hemmings BA. Inhibition of glycogen synthase kinase-3 by insulin mediated by protein kinase B. Nature 1995;378:785–9.

Cancer Research
The Journal of Cancer Research (1916–1930) | The American Journal of Cancer (1931–1940)

AACR American Association for Cancer Research

# Sonic Hedgehog Signaling Pathway Is Activated in ALK-Positive Anaplastic Large Cell Lymphoma

Rajesh R. Singh, Jeong Hee Cho-Vega, Yogesh Davuluri, et al.

*Cancer Res* 2009;69:2550-2558. Published OnlineFirst February 24, 2009.